Renewable Energy 68 (2014) 853–867

Contents lists available at ScienceDirect

Renewable Energy

journal homepage: www.elsevier.com/locate/renene

Steady-state analysis of a conceptual offshore wind turbine driven electricity and thermocline energy extraction plant

Daniel Buhagiar*, Tonio Sant

Department of Mechanical Engineering, University of Malta, Malta

ARTICLE INFO

Article history:
Received 5 July 2013
Accepted 21 February 2014
Available online

Keywords:
Offshore engineering
Hydraulic power
Wind turbine
seawater cooling

ABSTRACT

A system for using offshore wind energy to generate electricity and simultaneously extract thermal energy is proposed. This concept is based on an offshore wind turbine driven hydraulic pump supplying deep seawater under high pressure to a land based plant consisting of a hydroelectric power generation unit and heat exchanger. A steady-state system model is developed using empirical formulae. The mathematical model comprises the fundamental system sub-models that are categorised as the rotor, hydraulic pump, pipeline, hydroelectric turbine and heat exchanger. A means for modelling the seawater temperature field across a two-dimensional bathymetry is also discussed. These mathematical models are integrated into a computational tool and a brief parametric static analysis is undertaken. The results illustrate the effect of pipeline diameter, rotational speed of the grid connected hydroelectric turbine, and the turbine distance from shore on the overall performance of the system. Through adequate parameter selection, the total rate of energy output for such a system, consisting of both electricity and thermal energy, is shown to increase by as much as 84%, when compared to a conventional wind turbine having an identical rotor diameter but which supplies only electrical energy.

1. Introduction

Current offshore wind turbine designs are inherently based on conventional onshore turbine technology that has been adapted to the offshore environment [1]. Improvements have always been of an incremental nature, building gradually on existing and proven ideas. However, the marinisation of land-based technologies over the past decade has encountered a number of technical challenges as a consequence of the tough offshore environment. One issue is related to the mechanical transmission system of the turbine, where offshore gearbox failures are frequent. Existing offshore turbines often require a gearbox replacement after an average of 4 years in the field [2]. With the component contributing to around 10% of the wind turbine cost [2], such failures are highly detrimental to the viability of offshore wind. Problems are also being encountered on the electrical systems. The National Renewable Energy Laboratory (NREL) in the United States reports [3] that 27% of turbine repairs are due to electrical system failures, resulting from the requirement of sophisticated electronics in the nacelle. Although this also applies to onshore turbines, such maintenance in the offshore environment is substantially more expensive. Finally, existing electrical power transmission systems in offshore wind farms require large quantities of copper. Historically, copper prices have been very unstable [4], with substantial fluctuations having occurred in the past decade [5]. NREL lists the development of offshore specific technologies as a priority to maximise the value of offshore wind generation [6].

1.1. Hydraulic-based wind turbines

A concept that is being investigated in a bid to develop an offshore specific turbine involves a shift to a hydraulic-based transmission system [7], in which a large positive-displacement pump and a hydraulic pipeline would replace the gearbox and generator. A number of manufacturers have starting developing prototypes in this direction [8–10]. Some are opting for hydrostatic transmission systems [8,9], while a particular manufacturer is proposing a hydrodynamic system [10]. However, these prototypes still have a high dependency on nacelle-based components and almost all of them focus on only eliminating the gearbox. They still depend on a turbine-based generator, and make no attempt to centralise the process involving electricity generation.

A revolutionary concept comes from Delft University of Technology, where a hybrid closed- and open-loop transmission system is being proposed; the open-loop transmission system

* Corresponding author.
E-mail address: daniel.buhagiar.08@um.edu.mt (D. Buhagiar).

http://dx.doi.org/10.1016/j.renene.2014.02.043
0960-1481/

Nomenclature

c_p	specific heat capacity of seawater
c_{p-DS}	specific heat capacity of district system fluid
C_{P-max}	rotor maximum power coefficient
$C_{P-overall}$	OWTEP system overall power coefficient
D_i	pipeline internal diameter
D_o	pipeline outer diameter
D_{rotor}	rotor diameter
e	pipeline internal surface roughness
f	pipeline friction factor
h_i	heat transfer coefficient at the pipeline inner surface
h_o	heat transfer coefficient at the pipeline outer surface
k_{pipe}	pipeline material thermal conductivity
K	torque-angular velocity coefficient
L_{pipe}	pipeline length
$L^{(k)}$	pipeline elemental length
M_{Pelton}	torque generated by Pelton wheel shaft
M_{pump}	pump torque input
M_{rotor}	rotor torque output
p_{bp}	parasitic pressure load induced by boost pump at turbine base
p_{fr}	pipeline frictional pressure load
p_{nom}	pump nominal pressure load
$P_{no-load}$	pump power consumption at no pressure load
$p_{Pelt-elev}$	pressure head equivalent to Pelton wheel elevation above sea level
$p_{Pelt-noz}$	Pelton wheel nozzle pressure
p_{pump}	pump pressure load
Q	volumetric flow rate through the system
Q_{DS}	volumetric flow rate through district system
R	rotor radius
R_p	Pelton wheel radius
R_{tot}	total resistance to heat transfer along the pipe radial direction
S_p	salinity of seawater (g/kg)
$T_{in,DS}$	district system fluid temperature at heat exchanger inlet
$T_{out,DS}$	district system fluid temperature at heat exchanger outlet
$T_{in}^{(k)}$	elemental inlet temperature
$T_{out}^{(k)}$	elemental outlet temperature
$T_{s,o}^{(k)}$	Elemental outer surface temperature
$T_{\infty}^{(k)}$	elemental surrounding temperature
U	wind speed at hub-height
U_{cut-in}	rotor cut-in wind speed
$U_{cut-out}$	rotor cut-out wind speed
U_{rated}	rotor rated wind speed
v_n	Pelton wheel nozzle velocity
V_p	pump volumetric displacement
$V_{p,max}$	pump maximum volumetric displacement
$V_{p,min}$	pump minimum volumetric displacement
ϕ_{opt}	Pelton wheel optimum bucket speed ratio
$\varphi^{(k)}$	pipeline elemental inclination angle
λ_{opt}	rotor optimum tip-speed ratio
η_{gen}	generator efficiency
η_{mech}	pump instantaneous mechanical efficiency
$\eta_{M,nom}$	pump nominal mechanical efficiency
$\eta_{V,nom}$	pump nominal volumetric efficiency
η_{shaft}	Pelton wheel driveshaft efficiency
ρ_{air}	air density
ρ_{DS}	density of district system fluid
ρ_{sw}	seawater density
μ_{sw}	seawater dynamic viscosity
$\omega_{no-load}$	pump angular velocity at no pressure load
ω_{nom}	pump nominal angular velocity
ω_{Pelton}	Pelton wheel angular velocity
ω_{rated}	rotor rated angular velocity
ω_{rotor}	rotor angular velocity

Dimensionless parameters

C_d	pump damping constant loss coefficient
C_f	pump frictional constant loss coefficient
C_s	pump slip constant loss coefficient
C_C	Pelton nozzle contraction coefficient
C_V	Pelton nozzle velocity coefficient
Pr	Prandtl number at the internal flow-pipe interface
$\overline{Nu}_{Di}$	circumferentially averaged Nusselt number at the internal flow-pipe interface, with internal diameter as length scale
$\overline{Nu}_L$	circumferentially averaged Nusselt number at the pipe-external flow interface, with elemental length as length scale
Re_{D_i}	pipeline flow internal flow Reynolds Number, with internal diameter as length scale
Ra_{D_o}	external, buoyancy driven flow Rayleigh Number, with external diameter as length scale
Ra_L	external, buoyancy driven flow Rayleigh Number, with elemental length as length scale

would use seawater as the working fluid [11,12]. The idea is to have individual wind turbines pumping pressurised seawater to a centralised hydroelectric conversion plant, which could also be located onshore. This concept is one of the first attempts at centralised electrical energy generation. By eliminating the direct connection between the generator and wind turbine rotor, it has been possible to propose novel control schemes that improve the power harvesting capabilities of the turbine at higher wind speeds. Other modifications to the design will be required to support more efficient operation at higher wind speeds [12,13].

1.2. Deep water source cooling

The current research presented in this paper draws inspiration from the novel hydraulic turbine concept described above. This concept can be readily integrated with Deep Water Source Cooling (DWSC) enabling thermal energy from the deep sea to be extracted in conjunction with electrical generation. By implementing a heat exchanger after the hydroelectric generation stage, the cold water extracted from the deep sea can be used to cool a secondary fluid utilised in a district cooling system.

District cooling combined with a source of deep seawater has been shown to be an effective means for handling multi-megawatt cooling loads. Such systems are particularly effective in regions having high cooling demands and access to a large body of water. Deep seawater provides a vast source of renewable thermal energy because its temperature tends to be independent of season. This renewable energy resource results from the thermal stratification phenomena occurring in deep seas whereby solar radiation in only absorbed at the upper seawater layers, with the deep seawater layers retaining a cool and stable

temperature across the year [14,15]. An intermediate layer, often referred to as the thermocline layer, separates these two thermally distinct regions. This layer is characterised by substantial temperature fluctuations that occur over relatively small variations in depth.

The present study uses meteorological data obtained for the Maltese Islands, located in the centre of the Mediterranean Sea. This is an ideal location for such an analysis given the hot summers and surrounding deep waters. Locations such as Malta would benefit from the extraction of cold seawater for cooling, as the peak energy demand originates from the substantial cooling requirement in the hot summer months [16]. Fig. 1 shows monthly variations of temperature with depth observed in a central Mediterranean region.

Existing DWSC systems require electrical energy to power the pumps that draw in the cold fluid. The current research is a first attempt to evaluate the concept of wind-powered DWSC systems using an entirely open-loop system. The system also includes the centralised generation of electricity. Such a concept, illustrated in Fig. 2, is given the term: Offshore Wind and Thermocline Energy Extraction (OWTEP) system.

The objectives of this paper are to:

- Describe the conceptual OWTEP system
- Illustrate the development of a steady-state mathematical model of such a system
- Present results from simulations carried out on a single-turbine OWTEP system

2. Methodology

A mathematical model of a single turbine OWTEP system was developed, consisting of a number of numerical sub-models, modelling the performance of the rotor, pump, pipeline, hydroelectric turbine, heat exchanger and the thermal gradients of the surrounding seawater.

2.1. Wind turbine rotor

The rotor is the means by which energy from the wind is extracted by the system. This analysis is based on the rotor design of the NREL 5 MW Reference Wind Turbine [17]. This 126 m diameter three-bladed rotor was selected to act as a reference point for comparison between the performance of traditional wind turbine designs and that of the proposed system. Previous work on hydraulic-based wind turbines has also made use of this rotor design [12,18–20]. Detailed information on the design and power performance characteristics of this rotor is available in Ref. [17]. Relevant characteristics are listed in Table 1.

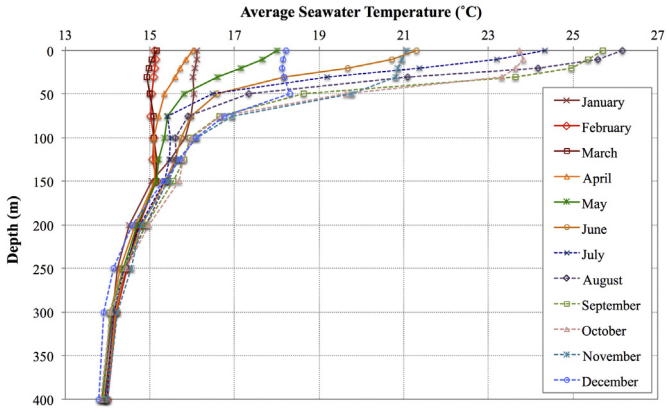

Fig. 1. Temperature–depth profiles for a central Mediterranean location.

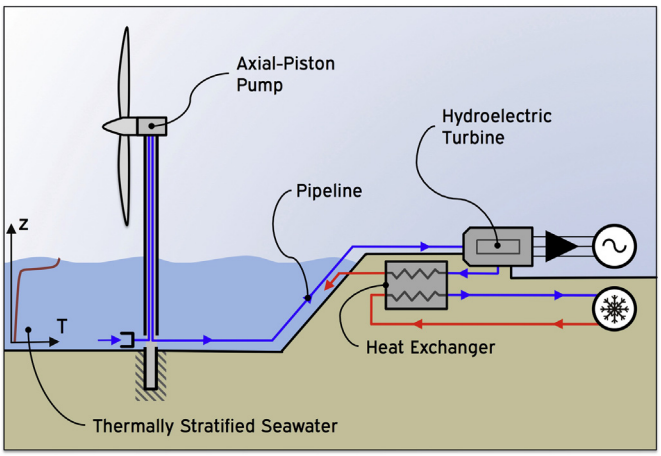

Fig. 2. Simplified schematic of the OWTEP System.

2.2. Nacelle-based positive-displacement pump

In the proposed design, the positive-displacement pump is directly connected to the rotor by a driveshaft. In order to optimise the rotor performance below the rated wind speed, as in traditional turbine control schemes, a means for controlling the torque of the rotor must be implemented. It has been shown [12,18], that by using a pump with a variable displacement the torque loading on the rotor can be continuously adjusted. One configuration is the swash-plate pump, which uses the motion of an inclined swash-plate to adjust the volume of fluid displaced per revolution. This method is analogous to generator torque control, as used in traditional wind turbines. However, it only requires a servo-controlled piston as opposed to the power electronic converters in current generator torque control systems [21].

An alternative approach used in a similar context is the combination of a radial-piston pump with the swash-plate pump, as discussed by Diepeveen [11] and Laguna [12]. This system uses a fixed-displacement radial piston pump for wind energy to hydraulic energy conversion, however, variable displacement is still required for rotor torque control, and this is undertaken by a swash-plate in a second fluid circuit within the hydraulic transmission system. An alternative means is the use of a digital displacement radial piston pump [9], which has variable displacement capabilities, however, such a concept is relatively new and adequately validated, "black-box" models of such pumps are not readily available. A single variable-displacement swash-plate pump was considered in this study as it is a well-understood pump design, which satisfies the functional requirements of the OWTEP system. Detailed hydraulic design considerations are beyond the scope of this work, but the aim is that positive results will motivate more elaborate development of this conceptual design.

Table 1
Selected parameters of the NREL 5 MW reference wind turbine rotor.

Cut-in, cut-out wind speeds [$U_{cut\text{-}in}$], [$U_{cut\text{-}out}$]	3 m s^{-1}, 25 m s^{-1}	Rotor diameter [D_{rotor}]	126 m
Rated wind speed [U_{rated}]	11.4 m s^{-1}	Rated rotor rotational speed [ω_{rated}]	12.1 rpm
Optimum tip–speed ratio [λ_{opt}]	7.55	Optimum power coefficient [$C_{p\text{-}max}$]	0.482

The modelling of a swash-plate pump is based on the method of lumped-parameters, as developed by Dasgupta and Mandal [22]. A model of an ideal pump is first proposed, from which the mechanical and volumetric efficiencies of the pump are defined. These efficiencies are then described in terms of three coefficients that individually describe the slip, damping and frictional losses within the pump. By definition, these coefficients are constant throughout the entire operating range of the pump [22]. They can therefore be obtained from known operating conditions, which typically correspond to the nominal and no-load conditions. For existing pump designs these are readily available from the pump manufacturer.

The proposed hypothetical system would require a pump capable of delivering hydraulic power in the region of 5 MW. The set points for such a pump were defined based on the nominal characteristics of the system observed in preliminary simulations and the typical efficiencies of positive displacement pumps [12,23–25]. The parameters for the OWTEP system pump are shown in Table 2. Note that the maximum and minimum volumetric displacements correspond to the nominal and no-load conditions respectively.

A boost pump must also be included at the base of the turbine, since the fluid cannot be pumped to hub height by suction. This pump draws power from the high-pressure line and uses it to induce a pressure increase on the low-pressure side, which is sufficient to pump the fluid up to the nacelle. Its effect on the resulting performance of the system is shown to be minimal. However, it is still considered in the analysis, as it is a fundamental mechanical component, without which the system cannot work.

2.3. Transmission pipeline

When designing transmission systems for hydraulic wind turbines for electrical generation only, the pipeline is designed to efficiently carry the fluid from the turbine to the hydroelectric conversion platform, minimising the frictional losses as far as possible. In this case, the pipeline must also transport thermal energy extracted from the deep sea, hence heat transfer across the pipeline walls should also be minimised. The modelling of the pipeline therefore consists of a steady-state model of the non-linear frictional loads along with a much more comprehensive thermal model.

2.3.1. Transmission pipeline: friction model

The frictional load induced on the pump by the pipeline is computed using the Darcy–Weisbach formula [26]:

$$p_{\mathrm{fr}} = \frac{8 f L_{\mathrm{pipe}} \rho_{\mathrm{sw}}}{\pi^2 D_{\mathrm{i}}^5} Q^2 \tag{1}$$

In equation (1), f is the friction factor of the pipeline. For laminar flows ($Re_{D_{\mathrm{i}}} < 2300$), f is equal to $64/Re$ [26]. In the case of turbulent flows, the more complex Colebrook and White [27] formula is often utilised. However, in this formula, the friction factor is expressed implicitly. This implies that when implemented into a computational algorithm, the friction factor cannot be found directly and some iterative procedure is typically used. In the current work, the Haaland approximation [28] is incorporated to obtain an explicit formula for the friction factor, shown in equation (2). This approximation is utilised in a number of simulation software packages as it can substantially increase the efficiency of the code [29].

$$f = \left[-1.8 \log\left(\frac{6.9}{Re_{D_{\mathrm{i}}}} + \left(\frac{e/D_{\mathrm{i}}}{3.7} \right)^{1.11} \right) \right]^{-2} \quad (Re_{D_{\mathrm{i}}} \geq 2300) \tag{2}$$

Table 2
Parameters of a conceptual OWTEP system pump.

Nominal pressure load [p_{nom}]	150 bar
Nominal angular velocity [ω_{nom}]	12.1 rpm
Mechanical efficiency at nominal conditions [$\eta_{\mathrm{M,\ nom}}$]	97%
Volumetric efficiency at nominal conditions [$\eta_{\mathrm{V,\ nom}}$]	98%
Angular velocity at no load [$\omega_{\mathrm{no\text{-}load}}$]	50 rpm
Power consumption at no load [$P_{\mathrm{no\text{-}load}}$]	30 kW
Maximum volumetric displacement [$V_{\mathrm{p,\ max}}$]	1.5 m^3/rev
Minimum volumetric displacement [$V_{\mathrm{p,\ min}}$]	0.05 m^3/rev

2.3.2. Transmission pipeline: thermal model

With respect to the thermal aspect, the pipeline consists of an internal forced convection problem, having a known inlet temperature and flow rate. The internal flow occurs in a solid cylindrical structure submerged in a static fluid having a continuously changing temperature. As a result of these temperature variations on the outside of the pipe, a finite-element method was utilised to model the pipe.

The pipeline geometry is discretised into one-dimensional elements as shown in Fig. 3. Each element has an inlet and outlet temperature, and a surrounding fluid temperature that is treated to be constant for each finite element. Heat transfer processes are categorised into internal forced convection, conduction and external free-convection. Conduction is modelled by the application of Fourier's law of conduction to a radial system. The thermo-fluidic properties of seawater are calculated for each element using correlations developed by Sharqawy et al. [30].

Internal forced convection is modelled using the Gnielinski empirical formula [31] (equation (3)), which gives the Nusselt number at the internal flow–pipeline interface. This correlation carries an associated uncertainty of 10% on the Nusselt number, as opposed to 25% as in more typically used correlations [32]. The improved accuracy comes at the cost computing the friction factor, although in this case it is readily available from the mechanical solution of the pipeline model.

$$\overline{Nu_{D_{\mathrm{i}}}} = \frac{(f/8)(Re_{D_{\mathrm{i}}} - 1000) Pr}{1 + 12.7 (f/8)^{1/2} (Pr^{2/3} - 1)} \tag{3}$$

External free convection is modelled using a set of recently published correlations (equation (4)) by Heo and Chung [33]. These correlations allow for obtaining the Nusselt number at the pipeline–external flow interface for different values of the pipeline

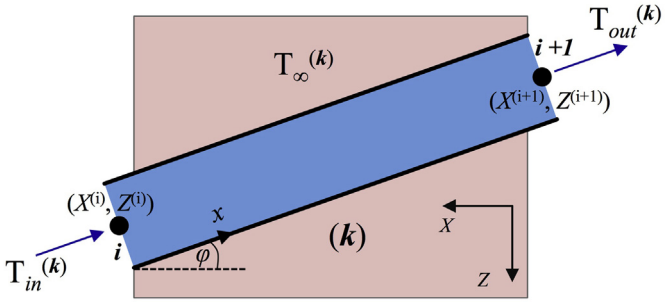

Fig. 3. A single pipeline element.

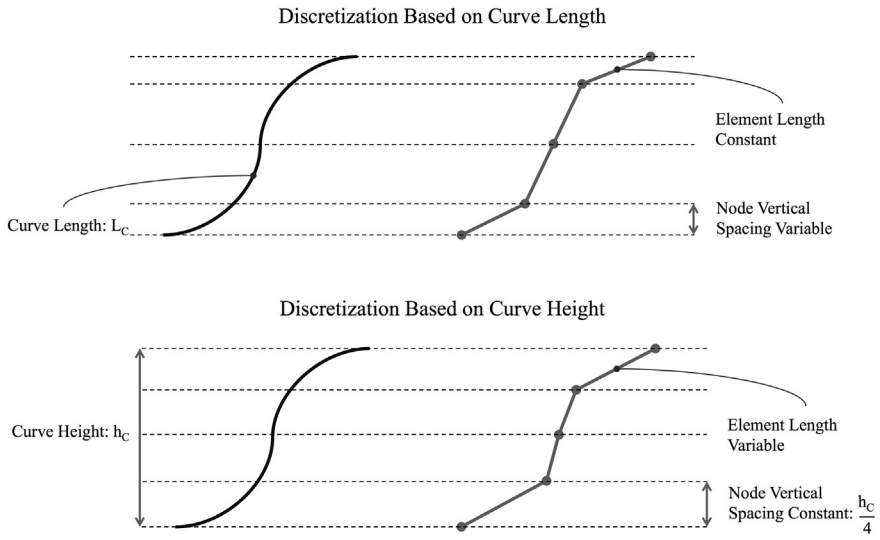

Fig. 4. Discretisation based on vertical height versus discretisation based on curve length.

inclination angle. Typical correlations had focused only on vertical [34] and horizontal [35] configurations. The nature of the external flow is described by the value of the Rayleigh number. This dimensionless quantity encompasses the ratios of buoyancy to viscous forces as well as molecular to thermal diffusivity [32]. It is the product of the Grashof and Prandtl numbers. The discontinuity in equation (4) corresponds to the laminar to turbulent transition of the external buoyancy driven flow. The angle $\varphi^{(k)}$ is the inclination angle of the pipeline element, measured in degrees from the horizontal position.

$$\overline{Nu_L} = \begin{cases} 0.67\mathrm{Ra}_L^{0.25}\left(1+1.44\mathrm{Ra}_{D_o}^{-0.04}\cos\varphi^{(k)}\right) & \mathrm{Ra}_L < 10^9 \\ 0.26\mathrm{Ra}_L^{0.28}\left(1+1.89\mathrm{Ra}_{D_o}^{-0.044}\cos\varphi^{(k)}\right) & \mathrm{Ra}_L \geq 10^9 \end{cases} \quad (4)$$

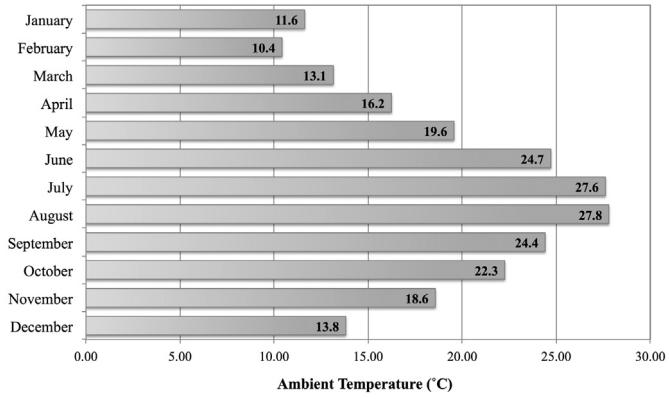

Fig. 5. Monthly average temperatures for Malta in 2012. Courtesy of the meteorological office at the Malta International Airport.

2.3.3. *Boundary conditions for the pipeline thermal model*

The boundary conditions of the pipeline thermal model are obtained from the surrounding seawater temperatures. These temperatures are obtained from the temperature field across the bathymetry. In this work, a two-dimensional bathymetry between the turbine position and the shoreline was considered.

The coordinates of the bathymetry are defined as distance from shore (X) and depth (Z). The final bathymetry is then constructed using a cubic-interpolation between the known coordinates to generate the curve with a resolution of 1 m in the X direction. In the work a simple parabolic bathymetry was considered, however the model is designed to receive adequately defined sets of coordinates corresponding to any desired profile.

The pipeline geometry is constructed primarily based on the bathymetric profile. The height at which the pipeline sits on the seabed is defined and a simple translation of the bathymetry

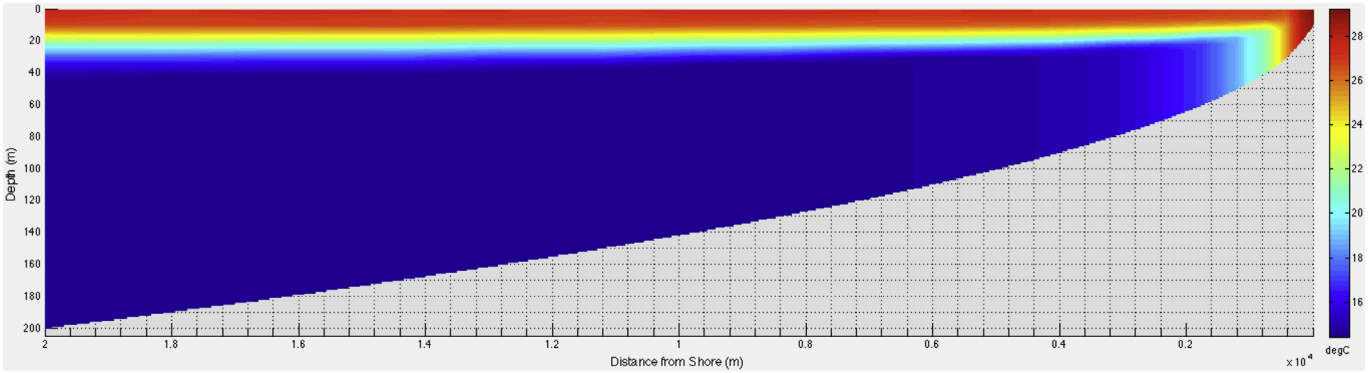

Fig. 6. Temperature field over a parabolic bathymetry for the month of August.

coordinates is carried out. The final geometry of the pipeline is obtained using the distance of the wind turbine from shore as well as the hub height and the spacing between the inlet and outlets of the turbine.

The pipeline is divided into finite elements using a vertical discretisation scheme. Such a scheme automatically refines the elements in steeper regions by fixing the vertical height of the elements, rather then their overall length. This is illustrated in Fig. 4. This is ideal given that the sharper fluctuations in temperature tend to occur across these elements. The pipeline under investigation was discretised into 5317 elements, which varied in length from 0.04 m to 28.87 m, depending on the rate of external temperature variation with depth in that region. The inclination angle of each element is computed by applying simple trigonometry to the nodal coordinates. This angle is required for computing the external Nusselt number.

The two-dimensional temperature field is obtained as a combination of the one-dimensional temperature–depth profiles for individual water columns. The numerical model of a one-dimensional water column, developed by Sharples et al. [14], was used to simulate the process of stratification. The details of this model will not be discussed further but can be found in Ref. [14]. In this context, its main function is to convert meteorological data into temperature–depth profiles corresponding to each depth in the temperature field.

The Meteorological Office at Malta International Airport provided the meteorological data used in this study; this data corresponds to the year 2012. Parameters required to implement this method are daily averaged values of: *ambient temperature, total solar radiance, atmospheric pressure, relative humidity, wind speed* and *wind direction*. Monthly average ambient temperatures for 2012 are shown in Fig. 5.

The hydrothermal model of the seawater column uses this data as boundary conditions to generate the daily temperature–depth profiles with a resolution of 1 m in the *Z*-direction. These profiles are then arranged according to the defined bathymetry to form the two-dimensional temperature field. In this study, twelve temperature fields were generated, corresponding to the 15th day of each

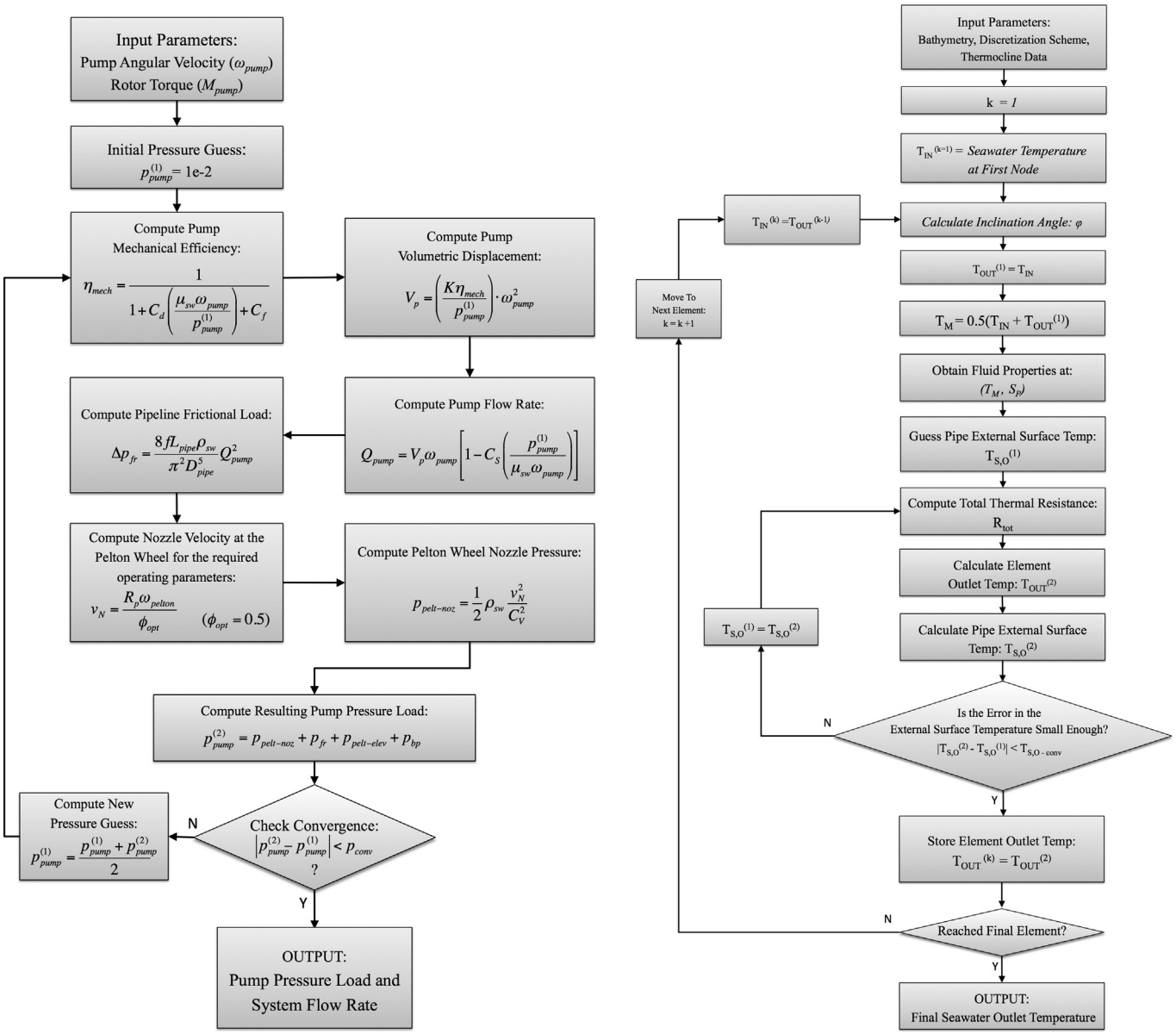

Fig. 7. Flowcharts for solution of the mechanical system and pipeline thermal model.

month. The temperature field for the month of August over a parabolic bathymetry is shown in Fig. 6.

The discretised pipeline geometry is superimposed onto the temperature depth profiles. The seawater temperature at each nodal location is obtained from the coordinates of each node. A two-dimensional, linear interpolation between neighbouring points on the temperature field was used to obtain values at the exact nodal positions. The elemental surrounding temperatures are computed as the arithmetic mean of the corresponding nodal temperatures.

2.4. Hydroelectric turbine

The pressurised seawater is converted into electricity by passing it through a hydroelectric turbine, which in this case is located onshore. Previous work by Diepeveen [36] has shown that given the pressure and flow characteristics of such a hydraulic transmission system, a vertical-axis Pelton wheel-type hydroelectric turbine is ideal.

The method for modelling the Pelton wheel uses a set of equations to describe the pressure requirement at the nozzle, along with the resulting shaft torque and hydraulic efficiency. A Pelton wheel directly coupled to a grid-connected generator must rotate at a constant velocity in order to supply electricity at the grid frequency. The hydraulic efficiency of a Pelton wheel is a function of numerous design parameters, such as the velocity coefficient of the nozzle and the ratio of the Pelton wheel bucket velocity to the jet velocity [37]. The latter parameter is referred to as the bucket speed ratio, for a fixed rotational speed, it tends to vary depending on the power available in the fluid. It can be shown that the Pelton wheel reaches its theoretical optimum hydraulic efficiency for a bucket speed ratio of 0.5, in practice this tends to be reached at a value of around 0.48 [37]. In the OWTEP system it is proposed that a servo controlled spear valve is utilised to continuously adjust the nozzle area and therefore the fluid velocity. This allows for continuously optimising the hydraulic efficiency of the Pelton turbine by maintaining a fixed nozzle velocity throughout the operation of the system while allowing the flow rate to vary subject to the intermittency induced by the wind turbine driven pump [38]. This concept is mathematically illustrated in Section 3.1.

In order to simplify the steady-state model, the electrical generator and driveshaft are modelled as having fixed efficiencies throughout their operation.

2.5. Heat exchanger

As indicated in Fig. 2, the thermal energy extracted from the deep sea is transferred to a fresh water circuit that is used in the district cooling system. The energy transfer process occurs in a heat exchanger that is located after the Pelton turbine. A small pump would most likely be required to circulate the fluid through the heat exchanger however its electrical demand would be negligible compared to the power generated by the system, is therefore neglected in the calculations. A simple counter-flow heat exchanger is used in this analysis [39]. This is modelled using the standard Number of Transfer Units (NTU) method, as described by Incropera et al. [32].

3. Steady-state system model

A computational tool was developed to model the performance of the OWTEP system. This combines the algorithms that correspond to the mathematical models of the various sub-systems. The theoretical formulation of each model is briefly described in this section.

3.1. Mechanical system model

The rotor was modelled using discontinuous functions of angular velocity (equation (5)) and torque (equation (6)) with respect to wind speed. The discontinuities correspond to changes in the control strategy, which in practice correspond to different operating conditions of the rotor based on the wind speed.

In this approach the intermediate control regions pertaining to the original NREL reference turbine were neglected. These regions of control are implemented between the discontinuities shown in (equation (5)) and have some effect on the torque-angular velocity relationship for very narrow regions of wind speeds. They were not included to simplify the model, but result in the rated maximum tip-speed of 80 m s^{-1} being exceeded by an additional 5 m s^{-1}. However, the understanding is that there is a minimal effect on the rotor power curve [17]. The intention is that with an improved understanding of the current system, intermediate regions will be included in the future to specifically describe a hydraulic-based transmission, unlike those described in Ref. [17], which relate to the behaviour of a rotor-driven induction generator.

$$\omega_{\text{rotor}}(U) = \begin{cases} 0, & [U < U_{\text{cut-in}}] \\ \left(\frac{\lambda_{\text{opt}}}{R}\right) U, & [U_{\text{cut-in}} \le U < U_{\text{rated}}] \\ \left(\frac{\lambda_{\text{opt}}}{R}\right) U_{\text{rated}}, & [U_{\text{rated}} \le U < U_{\text{cut-out}}] \\ 0, & [U \ge U_{\text{cut-out}}] \end{cases} \tag{5}$$

$$M_{\text{rotor}}(U) = K\omega_{\text{rotor}}^2 \tag{6}$$

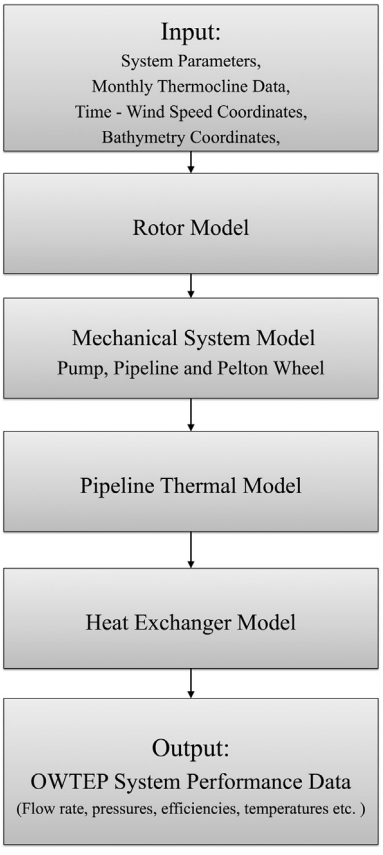

Fig. 8. Flowchart for solution of the system model.

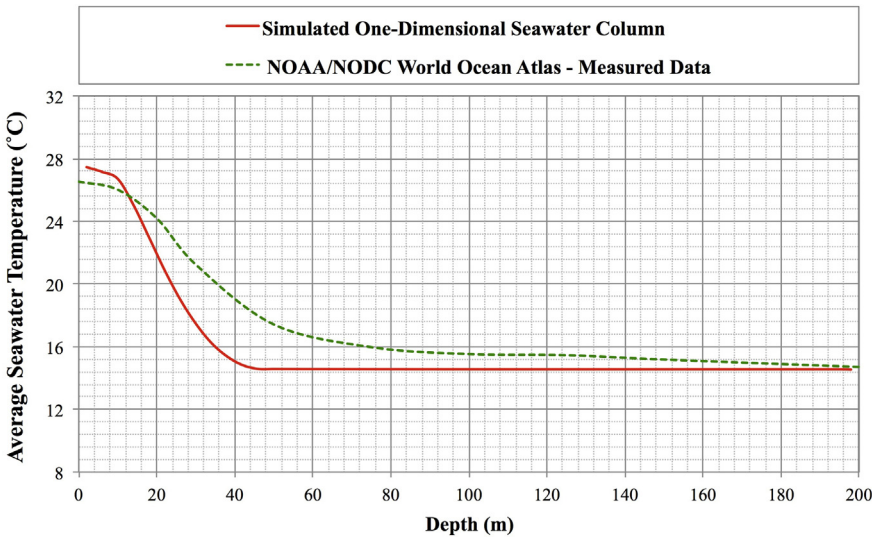

Fig. 9. Simulated temperature profile versus temperature profile from the NODC live Access server.

For steady-state conditions, it may be assumed that the torque developed by the rotor and that driving the pump is equal. By using a variable displacement pump, the torque loading on the pump may be optimised accordingly depending on the rotor operating state. The role of the constant K in equation (6) is to represent the relationship between the torque generated by the rotor and torque requirement of the pump. This concept is discussed by Laguna [12]. Equation (7) can be derived to give the numerical value of K for known rotor parameters.

$$K = \frac{1}{64\lambda_{opt}^3}\rho_{air}\pi D_{rotor}^5 C_{P-max} \tag{7}$$

The application of the method of constant loss coefficients results in equations (8) and (9), which describe the steady-state performance of the pump. The constant loss coefficients (C_d, C_f and C_s) can be obtained from the pump parameters (Table 2) using the method described by Dasgupta and Mandal [22].

$$M_{pump} = V_p p_{pump}\left[1 + C_d\left(\frac{\mu_{sw}\omega_{pump}}{p_{pump}}\right) + C_f\right] \tag{8}$$

$$Q = V_p\omega_{pump}\left[1 - C_s\left(\frac{p_{pump}}{\mu_{sw}\omega_{pump}}\right)\right] \tag{9}$$

The volumetric displacement of the pump that induces a torque loading which optimises the aerodynamics of the rotor is given by equation (10).

$$V_p = K\left(\frac{\eta_{mech}}{p_{pump}}\right)\omega_{rotor}^2 \tag{10}$$

Equation (10) implies that the volumetric displacement of the pump must be continuously adjusted based on the operating mechanical efficiency (η_{mech} is not a constant), the pump pressure load (Δp_{pump}) and the rotor angular velocity (ω_{rotor}). The selected pump should have a maximum volumetric displacement that corresponds to the rated wind speed since the pump torque loading is only used to optimise the rotor below the rated condition. This is further discussed in previous work [13]. Beyond this limit, rotor optimisation no longer takes place and angular velocity and/or torque can be adjusted using standard pitch control.

The driveshaft connecting the pump to the rotor was considered to be perfectly rigid and to induce negligible frictional losses. This implies that the rotor torque generated is entirely transferred to the pump, which results in equations (11) and (12).

$$\omega_{rotor} = \omega_{pump} \tag{11}$$

$$M_{rotor} = M_{pump} \tag{12}$$

The pressure load induced by the Pelton wheel nozzle is given by equation (13), which describes the non-linear, flow–pressure relationship across the nozzle orifice.

$$p_{pelt-noz} = \frac{1}{2}\rho_{sw}\left(\frac{v_n}{C_V}\right)^2 \tag{13}$$

The nozzle velocity required for optimum hydraulic efficiency and a constant angular velocity is calculated using equation (14). The nozzle area required to obtain this nozzle velocity is a function of the system flow rate, and can be obtained from equation (15). In practice, this area would be adjusted using the spear valve.

$$v_n = \frac{R_P\omega_{Pelton}}{\phi_{opt}} \tag{14}$$

$$A_N = \frac{Q}{C_C v_N} \tag{15}$$

The overall pressure load on the pump is given by equation (16). The term $p_{pelt-elev}$ corresponds to the head equivalent to the Pelton wheel elevation above sea level. The term Δp_{fr} is the frictional load described in Section 2.3 and p_{bp} is the parasitic pressure load induced by the boost pump at the base of the turbine. The efficiency of this boost system is taken to be fixed at 80%.

$$p_{pump} = p_{pelt-noz} + p_{pelt-elev} + p_{fr} + p_{bp} \tag{16}$$

Table 3
Default parameters of the steady-state OWTEP system model.

Pipeline	Turbine distance from shore	20 km
	Internal diameter (D_i)	0.5 m
	Thickness	25 mm
	Internal surface roughness (e)	0.4 mm
	Thermal conductivity (k_{pipe})	0.5 W m^{-1} K^{-1}
Pelton wheel	Pitch circle diameter	8 m
	Fixed Angular Velocity (ω_{Pelton})	200 rpm
	Elevation (above sea level)	20 m
	Shaft transmission efficiency (η_{shaft})	99% [36]
	Generator efficiency (η_{gen})	95% [36]
Heat exchanger	Effective area	1000 m^2
	U-value (no fouling)	1000 W m^{-2} K^{-1}
	District system flow rate (Q_{DS})	0.3 m^3 s^{-1}
	District system fluid density (ρ_{DS})	1000 kg m^{-3}
	District system specific heat capacity ($c_{p\text{-}DS}$)	4200 J kg^{-1} K^{-1}
	District system inlet temperature ($T_{in,\ DS}$)	25 °C
	Fouling factor	8.8 × 10^{-5} m^2 K W^{-1} [42]

3.2. Thermal modelling

The total resistance to heat transfer along the radial direction of the pipeline element is given by an arithmetic addition of the individual resistances (equation (17)). This derivation can be found in Ref. [32]. The outlet temperature of an element is obtained from equation (18). This equation follows from the derivation of the bulk fluid temperature of an internal flow, where a second fluid of known temperature surrounds the pipe.

$$R_{tot} = \frac{1}{\pi D_o h_o} + \frac{\ln\left(D_o/D_i\right)}{2\pi k_{pipe}} + \frac{1}{\pi D_i h_i} \tag{17}$$

$$T_{out}^{(k)} = T_{\infty}^{(k)} - \left(T_{\infty}^{(k)} - T_{in}^{(k)}\right)\cdot\exp\left(\frac{-L^{(k)}}{\rho_{sw} Q C_p R_{tot}}\right) \tag{18}$$

The model is solved starting from the element at the inlet. The outlet temperature of an element becomes the inlet temperature of the next element and the solution proceeds in this manner until the final element is reached. This outlet temperature corresponds to the outlet temperature of the pipeline. The temperature rise of the fluid as it passes through the pump was calculated to be negligibly small (≤0.2 °C), and is therefore not included in the model.

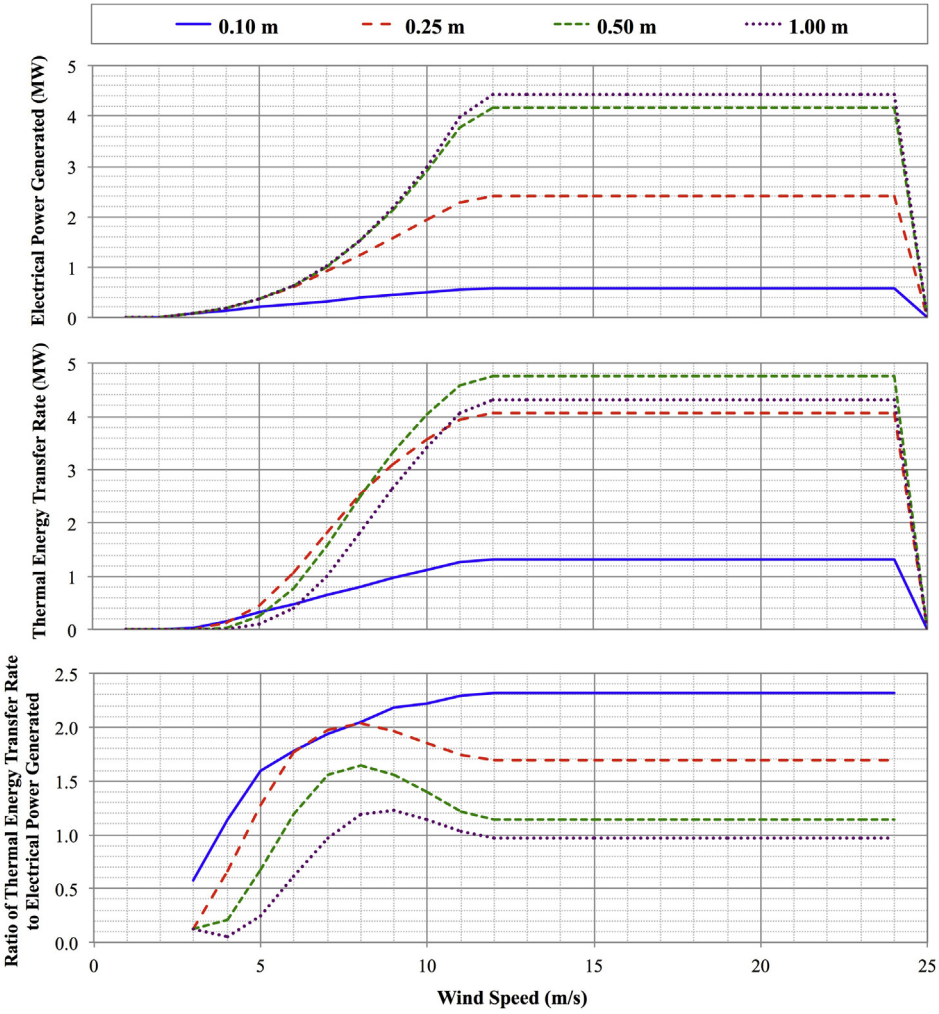

Fig. 10. The effect of internal diameter on the power and energy extraction characteristics of the turbine.

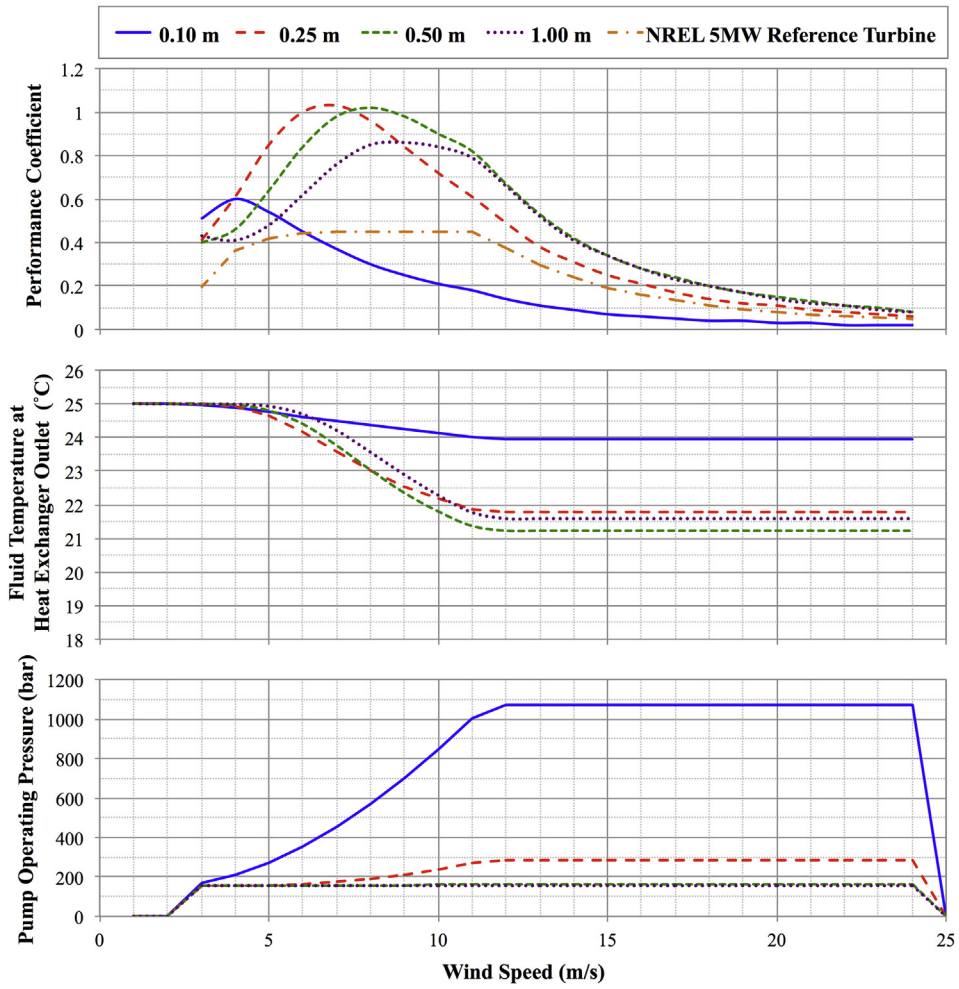

Fig. 11. The effect of internal diameter on selected operating parameters of the system.

3.3. Power output and the performance coefficient of the OWTEP system

Given the non-conventional generation capabilities of such a system are necessary to adequately define the total rate of energy generated. The resulting definition of the turbine performance coefficient must also be defined.

For such a wind turbine system, which is generating electricity while simultaneously extracting thermal energy, the input energy, which allows the system to function, is still that which is found in the wind stream passing through the rotor area. The energy output is the electricity generated in the Pelton wheel, which is computed by calculating the Pelton output shaft power and multiplying by the fixed generator efficiency. The thermal energy extracted is computed from the temperature change in the secondary fluid flowing through the district cooling system. The overall performance coefficient can therefore be obtained by dividing the total rate of energy delivered (consisting of electricity and thermal energy) by the power required to operate the system: the wind stream kinetic energy per second (equation (19)).

Admittedly, some additional power will be required in order to pump the fluid through the secondary loop comprising the district system. However, this depends on specific design aspects of the hydraulic circuit, which is beyond the scope of this work. Moreover, this additional power required for fluid circulation is expected to be orders of magnitude less than the input power coming from the wind stream kinetic energy.

3.4. Computational implementation

Both the mechanical and thermal aspects of the systems require iteration processes to compute the pressure loading and pipeline surface temperature respectively. These two algorithms are illustrated in Fig. 7. A flowchart containing all the computational algorithms in the sequence in which they are executed is shown in Fig. 8.

The computational model was programmed using the MATLAB® software package. MATLAB® (MATrix LABoratory) is a fourth-generation numerical computing environment [29]. In order to facilitate the analysis of the system and improve its usability a user-

$$C_{\mathrm{P-overall}} = \frac{M_{\mathrm{Pelton}}\omega_{\mathrm{Pelton}}\left(\eta_{\mathrm{shaft}}\eta_{\mathrm{gen}}\right) + \rho_{\mathrm{DS}}Q_{\mathrm{DS}}c_{\mathrm{p-DS}}\left(T_{\mathrm{in,\ DS}} - T_{\mathrm{out,\ DS}}\right)}{\frac{1}{2}\rho_{\mathrm{air}}\left(\frac{\pi D_{\mathrm{rotor}}^2}{4}\right)U^3} \tag{19}$$

interface was developed using the object-oriented environment: GUIDE [29], within the MATLAB© package. This allows for directly importing system parameters and other data files, as well as the visualisation and exporting of the results.

3.5. Verification and validation of the computational models

The OWTEP system model was verified by analysing the effect of convergence criteria and discretisation schemes. The aim of verification being to establish that the algorithms are not generating numerical errors and the solution is independent of the numerical aspects of the code. As part of the verification, it was also ensured that all empirical formulae for modelling thermo-fluid phenomena are applied within their limits of applicability.

3.5.1. Verification of the mechanical system model

The rotor model was shown to be in agreement with results from the NREL report [17] for the 5 MW reference turbine. The pump model was used to simulate the performance of off-the-shelf Bosch-Rexroth positive displacement pumps. The simulated behaviour was in excellent agreement with performance curves provided by the manufacturer [25], indicating that the model is working properly. Full-scale validation of the pump model using data for a 5 MW system is not currently possible since such data is not readily available. However, the method of Dasgupta and Mondal [22] has been shown to be adequate [12,36] for use with static models pertaining to hydraulic wind turbines.

3.5.2. Validation of the one-dimensional water column model

The applicability of the one-dimensional seawater column model was validated using data from the National Oceanography Data Centre (NODC) live access server [40]. Data for the waters surrounding the Maltese Islands was available in the form of averaged values of temperature with depth. The temperature–depth profile for a sea depth of 200 m was simulated using the water column model. The scope of the validation was particularly to establish if the water column model could successfully predict the year-round deep-water temperature, which is known to be around 15 °C. Following a calibration of the initial water temperature from within the model, the results agreed well with those from the NODC.

Fig. 9 shows the computed temperature–depth profile for the 16th day of August along with the NODC data for the same location and month. It must be noted that the computational model simulates the behaviour of single water column of a depth of 200 m using meteorological data for the year 2012. On the other hand, the NODC data consists of a set of objectively analysed climatological fields of temperature for a variety of depths [41], going up to 600 m, in the year 2000. Despite these two differences, the two results are in good agreement, particularly in terms of the deep-water temperature, which is the more comparable aspect of the data sets.

4. Results and discussion

A parametric analysis of the OWTEP system was carried out using the steady-state model. The aim of this analysis was to observe the effect of selected individual system parameters on the overall system performance.

The rotor and pump parameters shown in Tables 1 and 2 were used along with default system parameters shown in Table 3. The parabolic bathymetry shown in Fig. 4 was used along with temperatures for typical August weather in the Maltese archipelago. The month of August was selected as it corresponds to the country's annual peak energy demand [16] with an average ambient temperature of 27.8 °C.

4.1. Pipeline internal diameter

The pipeline internal diameter is a fundamental aspect of the system as it affects the pressure characteristics on the mechanical side, as well as the heat transfer characteristics of the pipeline.

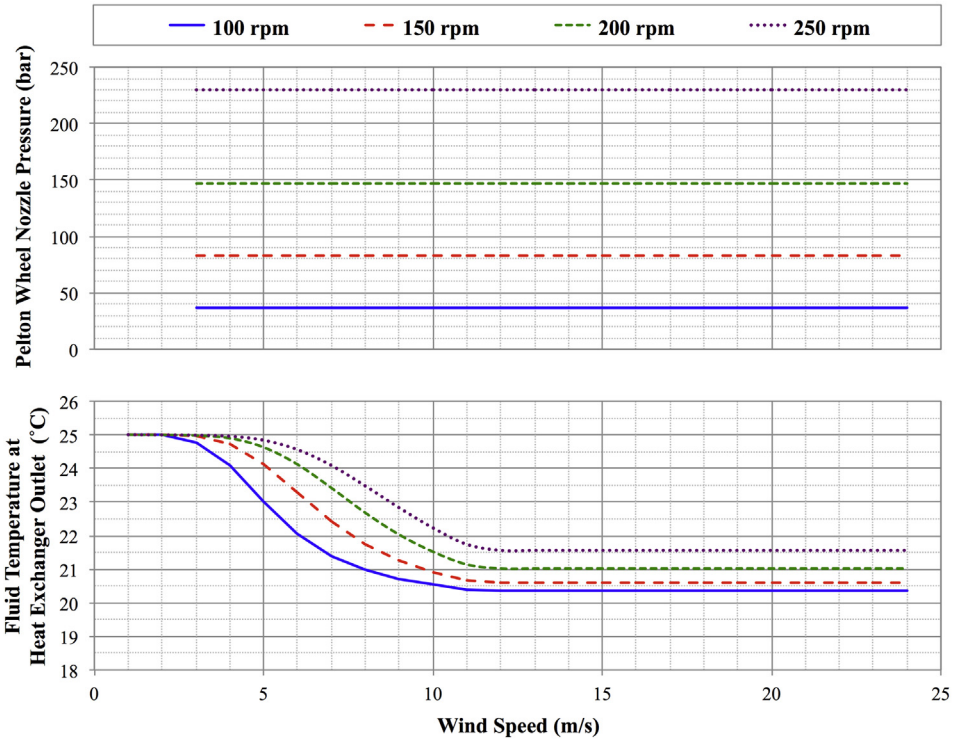

Fig. 12. The effect of Pelton wheel angular velocity on the nozzle pressure and the outlet temperature of the secondary fluid in the district system.

The output characteristics of the OWTEP system are shown in Fig. 10. The first aspect that can be noted is the substantial increase in power because of thermocline energy extraction. Moreover, the energy output is very sensitive to the internal diameter when this is relatively small. However, the effect of increasing this parameter beyond 0.5 m is negligible.

The variation of the performance coefficient with wind speed is very different to that observed for the same rotor control scheme on typical turbine designs (Fig. 11). Beyond a particular wind speed, the pipeline output temperature remains unchanged, and the heat exchanger reaches the maximum possible heat transfer rate (Fig. 11). This implies that as wind energy increases, thermal extraction tends to remain fixed. The electrical power output is also limited by the control scheme. The performance coefficient curve therefore tends to increase to a peak value after which it decreases as result of an increasing wind energy input and fixed electrical and thermal energy output. The optimum performance coefficient is observed for pipeline diameters in the region of 0.25–0.5 m. Increasing the diameter in this region has the effect of shifting the peak in curve to a higher wind speed. However, the effect of internal diameter on pipeline pressure (Fig. 1) implies that a 0.5 m diameter is much more efficient in terms of frictionally induced pressure loads. Smaller pipeline diameters are not feasible in this respect. On the other hand increases beyond 0.5 m have little to negligible effect. It can also be observed that the OWTEP performance coefficient for adequate pipeline diameters is superior to that of the NREL 5 MW reference turbine [17], which only generates electrical energy.

4.2. Pelton wheel angular velocity

A fixed rotational velocity of the Pelton wheel is crucial for a grid-connected power generation system. The numerical value of the angular velocity determines the frequency of the resultant alternating current generated from a directly connected synchronous machine. In the current analysis, the aim is to assess the effect of different Pelton wheel angular velocities on the system itself.

The main performance variation is in terms of nozzle pressure, which increases for higher angular velocities (Fig. 12). This implies that in order to transfer a fixed amount of hydraulic power, a lower flow rate is required. This has the advantage of reducing pipeline losses, but also reduces the rate of heat transfer in the heat exchanger (Fig. 12). Increasing the Pelton wheel angular velocity tends to increase power harvesting at lower winds speeds, although at above rated wind speeds the overall output power reaches the highest fixed level for 200 rpm (Fig. 13).

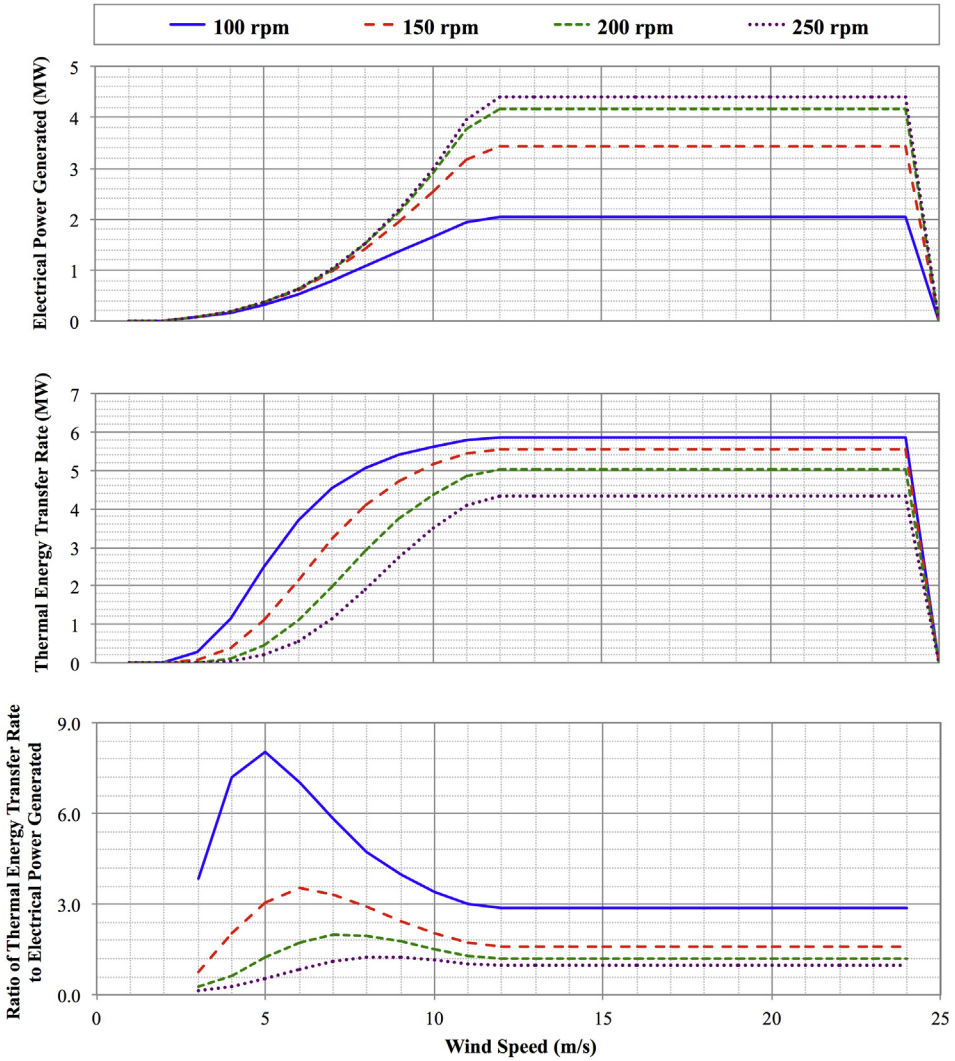

Fig. 13. The effect of Pelton wheel angular velocity on the power and energy extraction characteristics of the turbine.

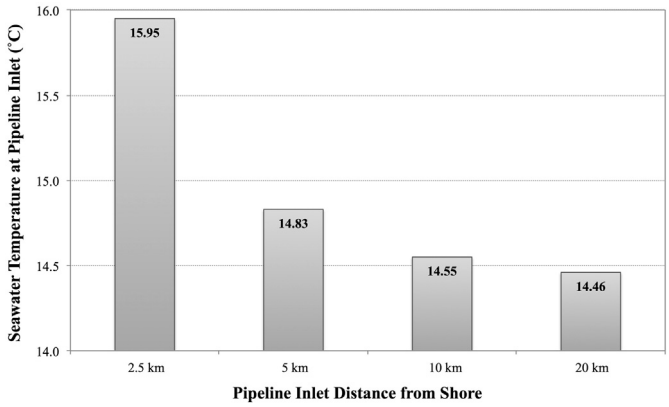

Fig. 14. Seawater inlet temperature variation with pipeline inlet distance from shore.

4.3. Turbine distance from shore

For a fixed parabolic bathymetry, the turbine distance from shore was adjusted in order to observe the simultaneous effect of extracting seawater from shallower regions along with a shorter pipeline. It must be noted that no consideration is made for the variation in wind quality with distance from shore.

As a result of the parabolic nature of the bathymetry and the position of the thermocline, the pipeline inlet temperature does not tend to vary substantially with distances beyond 5 km (Fig. 14). Although an appreciable difference of around 1 °C is observed when going from 2.5 to 5 km. The longer pipeline results in increased thermal losses, which indicate an ideal compromise between low inlet temperature and reduced losses can be struck at around 10 km (Fig. 15). The effect of pipeline length on the frictional pressure losses tends to be negligible for the selected default pipeline diameter of 0.5 m. This effect becomes more pronounced for smaller diameters.

4.4. Electrical generation

The electrical generation capability of an OWTEP turbine is observed to be inferior compared to that of a traditional wind turbine design. Fig. 16 shows the output electrical power from the OWTEP system along with data for the NREL 5 MW reference wind turbine [17]. These two results are directly comparable as a result of

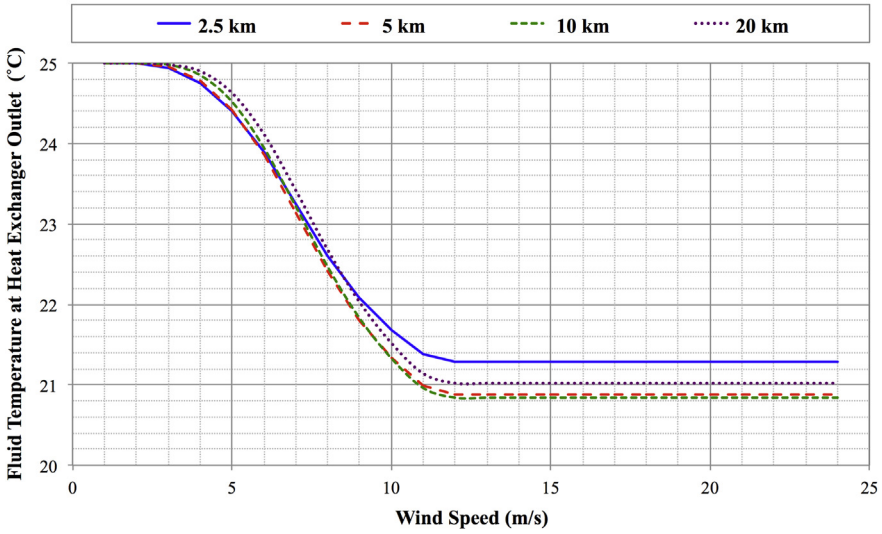

Fig. 15. The effect of turbine distance from shore on the outlet temperature of the secondary fluid in the district system.

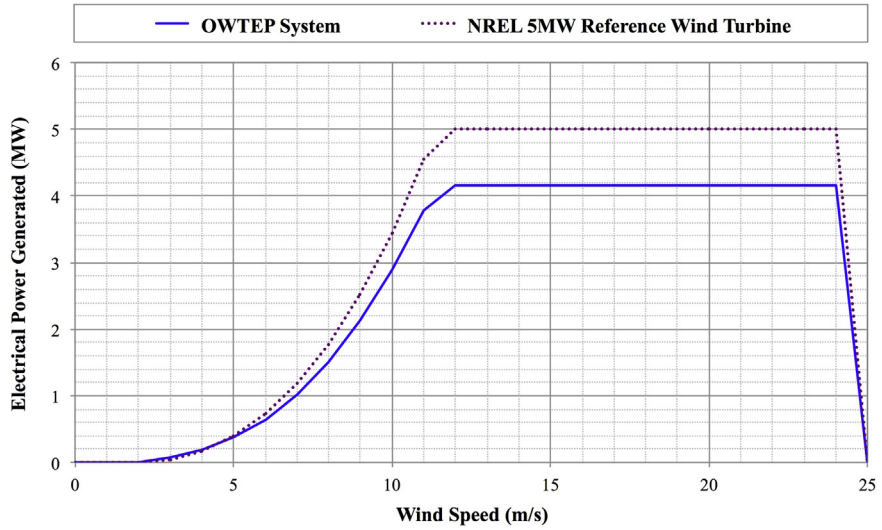

Fig. 16. Comparison between electricity generated by the OWTEP system and NREL 5 MW reference turbine.

the identical rotor and control scheme. However, it must be noted that the control scheme is designed for a traditional wind turbine having a generator-connected rotor in the nacelle. This scheme is designed to limit generator angular velocity and torque loading. In the case of the OWTEP system such a scheme is no longer relevant and alternatives can be considered. Moreover, the thermal extraction aspects of the system more than compensates for the decreased electrical output. It must also be noted that NREL data [17] corresponds to nacelle-generated electricity, which will experience losses as it is transmitted onshore. On the other hand, the OWTEP electricity is generated onshore.

5. Conclusions

The concept of an offshore wind turbine capable of generating electricity and simultaneously extracting thermal energy has been investigated. Results from the application of the steady-state model have shown that by selection of adequate parameters, the total power extracted at above rated conditions in the hot summer months can increase by as much as 84%. It has also been observed that the performance coefficient of such a system tends to experience a peak below the rotor rated wind speed. The value of this peak and the wind speed at which occurs has been shown to depend on the specific parametric values.

It must be noted that the dynamic behaviour of the system is not considered in this analysis. Transient aspects will affect the design and performance of the combined concept, particularly in terms of the instantaneous power production and the power quality. The aim of future work is to carryout a much wider, more comprehensive, parametric analyses. Further research involving transient models is required to examine the feasibility of using such long pipelines with a hydroelectric station onshore. Flow dynamics over long distances will cause lags in the pressure variation at the hydroelectric station with respect to wind speed variations. On the other hand, the hydraulic capacitance of a long pipeline may to a certain extent result in power smoothing. Moreover, this study has made no attempt to quantify the capital and operational costs (CAPEX and OPEX) of such a system. Such an analysis could provide a value for the cost of energy (€/kWh) and therefore a more fair comparison with existing wind turbine technologies. At this point, such a parameter is difficult to obtain given that the technology is still in early stages of development.

An additional consideration must be made for the possibility of using floating turbines in deep-sea regions. In this case the seawater pipeline system will be much more challenging to design, since it must accommodate the motion of the wind turbine with respect to the seabed. Addressing this matter was beyond the scope of this study.

In locations with high cooling demands such as Malta, most of the electrical energy is used for air-conditioning in the summer months [43]. A case study carried out by Sant and Farrugia [20] has already shown that the energy harvesting capability of such a system installed in Malta is substantially greater than those of traditional wind turbines. Through the application of a simplified steady-state model of an OWTEP system and using real wind data obtained for the central Mediterranean, the annual energy generation was shown to increase by 65.8% when compared to a traditional wind turbine having an identical rotor diameter and generating only electrical energy [20].

Despite the widely applied concept of DWSC and traditional wind energy generation, this system signifies the first attempt at a hybrid system. Its viability extends to locations with high cooling demands and adequate wind speeds that are adjacent to a suitably large body of water. Results indicate the potential for such a system as an offshore-specific wind turbine design. By widening the notion of wind-generated energy one can look beyond electrical generation and focus on generating energy in the form in which it is required, with the ultimate aim being to radically increase the viability offshore wind energy.

Acknowledgements

The authors would like to thank Mr. Joseph Schiavone from the meteorological office at the Malta International Airport for providing the data used in this research. The authors would also like to thank Prof. Jonathan Sharples of the University of Liverpool and the National Oceanography Centre in the UK, for permitting the use of a computational tool that simulates the temperature profiles across the one-dimensional water column.

References

[1] Diepeveen N. Seawater-based hydraulics for offshore wind turbines. Delft University Wind Energy Research Institute (DUWIND); 2009. Progress Report.
[2] Ragheb AM, Ragheb M. Wind turbine gearbox technologies. In: Carriveau R, editor. Fundamentals and advanced topics in wind power. InTech; 2011. pp. 189–206.
[3] Sheng S. Investigation of various wind turbine drivetrain condition monitoring techniques. In: Wind Turbine Reliability Workshop, USA; 2011. NREL/PR-5000-52352.
[4] Schmitz C. The rise of big business in the world, copper industry 1870-1930. Econ Hist Rev 1986;39:392–401.
[5] Ackerman R. A bottom in sight for copper. Forbes Inc.; Apr-2009.
[6] Hand MM, Baldwin S, DeMeo E, Reilly JM, Mai T, Arent D, et al. Renewable electricity futures study. USA: National Renewable Energy Laboratory; 2012.
[7] Diepeveen N, Van der Tempel J. Delft offshore turbines: the future of wind energy. Delft University of Technology; 2008.
[8] ChapDrive. ChapDrive [Online], http://www.chapdrive.com; 2011, August.
[9] Mitsubishi Power Systems Europe, Ltd.. SeaAngel: the future of offshore wind. London: Brochure; 2012.
[10] Voith Turbo Wind Gmbh & Co. KG. A unique solution to generating electricity from the wind: the WinDrive technology [Online], http://www.voith.com/en/products-services/power-transmission/variable-speed-gearboxes/windrive-technology-26688.html; 2009, May.
[11] Diepeveen N. Design considerations for a wind-powered seawater pump. In: European Offshore Wind Conference Proceedings, Stockholm; 2009.
[12] Laguna AJ. Steady-state performance of the delft offshore turbine. Delft: Faculty of Aerospace Engineering, Delft University of Technology; 2010. M.Sc. Thesis.
[13] Buhagiar D. Analysis of a wind turbine driven hydraulic pump. Malta: Department of Mechanical Engineering, University of Malta; 2012. B.Eng. Thesis.
[14] Sharples J, Ross ON, Scott BE, Greenstreet SPR, .Fraser H. Inter-annual variability in the timing of stratification and the spring bloom in the north-western North Sea. Cont Shelf Res 2006;26:733–51.
[15] Nakamura K, Hayakawa N. Modelling of thermal stratification in lakes and coastal seas. In: Hydrology of Natural and Manmade Lakes (Proceedings of the Vienna Symposium), vol. 26; 1991. Vienna.
[16] Enemalta. Annual report and financial statements. Enemalta Corp.; 2009–2011.
[17] Jonkman J, Butterfield S, Musial W, Scott G. Definition of a 5-MW reference wind turbine for offshore system development. Colorado: U.S. Department of Energy, National Renewable Energy Laboratory; 2009.
[18] Buhagiar D, Sant T. Performance analysis of a wind turbine driven swash plate pump for large scale offshore applications. EWEA – The Science of Making Torque from Wind, Oldenburg; 2012.
[19] Buhagiar D, Sant T. Analysis of a stand-alone hydraulic offshore wind turbine coupled to a pumped water storage facility. In: Sustainable Energy 2013: the ISE Annual Conference, Malta; 2013.
[20] Sant T, Farrugia R. Performance modelling of an offshore floating wind turbine-driven deep sea water extraction system for combined power and thermal energy production: a case study in a central Mediterranean context. In: ASME 32nd International Conference on Ocean, Offshore and Arctic Engineering, Nantes; 2013.
[21] Manwell J, McGowan J, Rogers A. Wind energy explained, theory, design and application. England: John Wiley & Sons; 2002.
[22] Dasgupta K, Mandal SK. Analysis of the steady-state performance of a multi-plunger hydraulic pump. Proc Inst Mech Eng Part J Power Energy 2002;206:471–9.
[23] Warring RH. The positive displacement pump, pumps: selection, systems and applications. Trade and Technical Press, Ltd.; 1984. pp. 65–103.
[24] Hamidat A, Benyoucef B. Mathematical models of photovoltaic motor-pump systems. Renew Energy 2008;33(5):933–42.
[25] Bosch Rexroth [Online]. Bosch Rexroth; 2012, November., http://www.boschrexroth.com/ics/Vornavigation/VorNavi.cfm?Language=EN&Region=none&PageID=Start.

[26] White FM. Fluid mechanics. 4th ed. Rhode Island, USA: McGraw Hill; 1998.
[27] Colebrook CF, White CM. Experiments with fluid friction in roughened pipes. Proc R Soc Lond Ser Math Phys Sci 1937;161(906):367–81.
[28] Haaland SE. Simple and explicit formulas for the friction factor in turbulent flow. J Fluids Eng 1983;105(1):89–90.
[29] MathWorks. Simscape users guide. Natick, MA: The MathWorks Inc.; 2010.
[30] Sharqawy MH, Lienhard JH, Zubair SM. Thermophysical properties of seawater: a review of existing correlations and data. Desalin Water Treat 2010;16:354–80.
[31] Gnielinski V. New equations for heat and mass transfer in turbulent pipe and channel flow. Int Chem Eng 1976;16:359–67.
[32] Incropera FP, DeWitt DP, Bergman TL, Lavine AS. Chapter 6: introduction to convection. Fundamentals of heat and mass transfer. 6th ed. New Jersey: John Wiley & Sons Inc; 2006. pp. 347–87.
[33] Heo JH, Chung BJ. Natural convection heat transfer on the outer surface of inclined cylinders. Chem Eng Sci 2012;73:366–72.
[34] Churchill SW, Chu HHS. Correlating equations for laminar and turbulent free convection from a vertical plate. Int J Heat Mass Transf 1975;18(11):1323–9.
[35] Churchill SW, Chu HHS. Correlating equations for laminar and turbulent free convection from a horizontal cylinder. Int J Heat Mass Transf 1975;18(9):1049–53.
[36] Diepeveen N. On the application of fluid power transmission in offshore wind turbines. Delft: Delft University of Technology; 2013. PhD Thesis.
[37] Thake J. The micro-hydro Pelton turbine manual: design, manufacture and installation for small-scale hydro-power. ITDG Publishing; 2000.
[38] Puleva T, Ichtev A. Adaptive multiple model algorithm for hydro generator speed and power control. Control of Power Plants; 2008.
[39] Kuppan T. Heat exchanger design handbook. New York: Marcel Dekker, Inc.; 2000.
[40] NODC. NODC live access server 7.3 [Online], http://data.nodc.noaa.gov/las/getUI.do; 2012, August.
[41] NODC. National oceanographic data centre [Online], http://www.nodc.noaa.gov/OC5/WOA09/pr_woa09.html; 2013, June.
[42] Welty JR, Wicks CE, Wilson GL, Rorrer GL. Fundamentals of momentum, heat and mass transfer. 5th ed. John Wiley & Sons, Inc.; 2000.
[43] Buhagiar V. Sustainable development and building design in Malta. Malta: Commonwealth Peoples Forum; 2005.